

# Photoelastic analysis of dynamic stress distribution around short implants restored with different materials

> **S. M. BURGOA-LA-FORCADA<sup>1</sup>, C. E. EDWARDS REZENDE<sup>2</sup>, C. CASTIGLIA GONZAGA<sup>2</sup>, J. CESAR ZIELAK<sup>2</sup>, A. YOSHIO FURUSE<sup>3</sup>**

<sup>1</sup> Graduate Student at Post Graduation Program of Clinical Dentistry, Positivo University, Curitiba, Brazil

<sup>2</sup> Full Professor at School of Dentistry, Positivo University, Curitiba, Brazil

<sup>3</sup> Full Professor at Bauru School of Dentistry, University of São Paulo, Bauru, Brazil

## TO CITE THIS ARTICLE

Burgoa-la-Forcada SM, Edwards Rezende CE, Castiglia Gonzaga C, Cesar Zielak J, Yoshio Furuse A. Photoelastic analysis of dynamic stress distribution around short implants restored with different materials. *J Osseointegr* 2018;10(2):44-49.

DOI 10.23805 /JO.2018.10.02.03

## ABSTRACT

**Aim** This study aimed at evaluating the stress distribution around a locking tapered short dental implant (4.3 mm x 6 mm), comparing crowns made of metal (CoCr), zirconium (Y-TZP) and acrylic resin.

**Materials and methods** The Y-TZP and resin crowns were fabricated by CAD/CAM system, while the CoCr crown was fabricated from lost wax technique. The implant was placed in a rigid photoelastic resin in order to analyze the stress distribution using a polariscope. An axial load starting at 0 (N) up to 200 (N) was applied at the center of the occlusal aspect of the crowns. The photoelastic models and the computer screen (where the data was exhibited) were recorded by video and the images were analyzed and compared at 50N, 100N, 150N and 200N loads.

**Results** It was observed that resin crown model generated lower stress around the implant.

**Conclusions** Resin crown generated best stress distribution around locking tapered short implant in comparison with Y-TZP and CoCr crowns.

**KEYWORDS** Zirconia, Dental Crowns, Dental Implants, Dental Prosthesis

## INTRODUCTION

Alveolar bone resorption after tooth extraction may limit bone volume availability for implant placement. The conventional treatment for this situation consists in surgical procedure for bone height augmentation, like bone grafting procedures. Currently, the use of short implants is considered as an alternative to solve these cases. Although the ability of short implants to support masticatory loads has been initially questioned, clinical and laboratory research has shown promising results (1-4).

The stress distribution in an implant system depends on many factors, like implant design, implant length, implant abutment joint, prosthesis and abutment design, restorative material and the forces and moments applied to the system (5-6). An overload on the implant system can cause stress concentration in the peri-implant bone and thus, if the stress intensity exceeds the physiological limits, there may be a stimulus to bone resorption so that a bone loss in the cervical third of the implant could be observed (5,7-8). This concentration of stress could be more critical in short implants, since the crown-implant ratio is biomechanically more challengeable and, furthermore, the area of stress dissipation generated by the masticatory load is reduced (8-10). On the other hand, clinical studies evaluating locking-tapered short dental implants with platform switching concept has shown favorable crestal bone maintenance (11-12).

Regarding the role of the prosthetic restorative material, despite some authors assert that more resilient materials with greater deformation capacity and impact reduction would have a damping effect, leading to a better distribution of stress (13), there are others stating that there is no influence of the materials used for the crown construction on the stress distribution around dental implants (14).

The aim of this study was to determine the stress distribution around short locking-tapered dental implants due to the restorative material used for cemented single

crown construction. Thus, the null hypothesis to be tested is: There is no influence of material used for crown construction on the pattern of stress distribution in the peri-implant bone around locking-tapered short dental implants.

## MATERIALS AND METHODS

### Specimens preparation

A premolar shaped crown was designed by the CAD software (Zirkonzahn.Modellier, Gais, Germany) generating a 3D virtual model of the specimens, which worked as a reference for milling two distinct crowns (M5 Heavy – milling unit, Zirkonzahn, Gais, Germany), one made of Yttria Tetragonal Zirconia Polycrystal (Y-TZP) (Prettau Zirconia, Zirkonzahn, Gais, Germany) and the other one made of acrylic resin (Temp basic, Zirkonzahn, Gais, Germany). The occlusal aspect of the crown had two flat sides converging to the midline, thus the central sulcus was located exactly in center of the plane perpendicular to the long axis of the crown.

A third metal crown was made by the lost wax technique from an acrylic resin replica (Duralay Reliance Dental Mfg Company Worth, Illinois, USA) obtained by the impression of the Y-TZP crown using a silicone material (Zetaplus e Oranwash, Zhermack - Labordental, São Paulo, Brazil). The casting was carried out with CoCr alloy (Fit Cast Cobalto, Talmax, Curitiba/PR, Brazil).

Three sets composed by universal conical abutments for cemented prosthesis attached onto locking tapered short implants (6mm height and 4.3mm width - Kopp, Curitiba, Brazil) using platform switching concept (Fig. 1) received the metal, Y-TZP and acrylic resin crown, respectively (Fig. 2). The crowns were cemented with a resin cement (Multilink, Ivoclar Vivadent, Schaan, Liechtenstein), according to the manufacturer's recommendations. The Y-TZP and metal crowns received internal conditioning with Primer for metal and Y-TZP supplied by the manufacturer (Metal/Zirconia Primer, Ivoclar Vivadent AG, Schaan, Liechtenstein). The abutments also received this same treatment. The resin crown received no conditioning. Afterwards, equal parts of cement were mixed for 30 seconds and the cement was inserted into the crown. The crowns were seated onto the abutments and the cement excess was immediately removed. All specimens showed resistance to manual traction 10 minutes after cementation.

### Photoelastic model construction

four glass plates were fixed in lower part of a verticulator forming a glass box. A guide was fixed to the upper part of the verticulator to guarantee the specimens positioning perpendicular to the horizontal plane. Thus, a rigid epoxy resin (Resina Rígida G IV; Polipox, São Paulo, SP, Brazil) was prepared according to the manufacturer's instructions and slowly inserted into the box glass, generating a



FIG. 1 Locking tapered implant (left) and the universal abutment for cemented crown (right).



FIG. 2 Specimens composed of short locking tapered implants, universal titanium abutment and Y-TZP (left), acrylic resin (middle) and CoCr (right).



FIG. 3 Photoelastic model placed in the universal testing machine to receive the axial load at the center of the occlusal aspect.

photoelastic model simulating a situation in which the implant was placed at the crestal bone level. After 24h hours from the epoxy resin preparation, the photoelastic models were evaluated in the polariscope (Optovac, Osasco, SP, Brazil) to verify the presence of residual stress.

### Stress distribution tests

For the tests, the photoelastic models were placed on a support and taken to the polariscope coupled to a

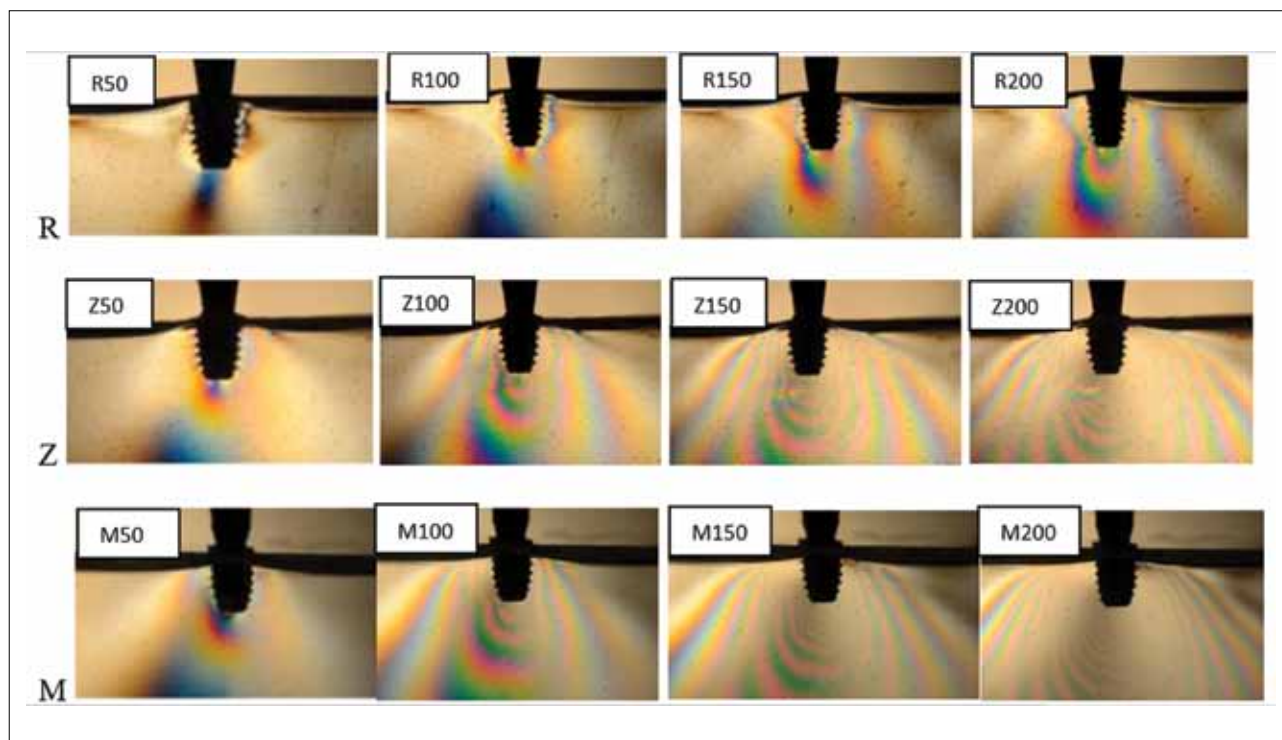


FIG. 4 Isochromatic fringe patterns for the different models under different loads. The higher number of fringes showed higher stresses for the metal and Y-TZP models. The proximity of fringes also indicates higher stress concentrations for the metal, followed by Y-TZP, with resin model showing less stress concentration. R: Resin - Z: Y-TZP - M: Metal

universal testing machine (DL2000; Emic, São José dos Pinhais, PR, Brazil). The specimens composed by the sets crowns/abutments/implants were subjected to compressive axial loads ranging from 0 to 200N with a speed of 0.5 mm/min at the center of the occlusal aspect of the crown. A spherical piston with 3 mm diameter was used as antagonist.

A camcorder in high definition (HD) was used to record the test (D7000; Nikon, Tokyo, Japan; Micro Nikkor 105 mm lens), while a second camcorder (FZ47, Lumix, Tokyo, Japan) was used to record the computer screen where the data was displayed. In order to standardize the capture of images, the camera was adjusted to manual focus, aperture (f/9), speed (1/60) and ISO (400). The white balance was kept in automatic mode.

The photoelastic stress fringes showed by each model were visually monitored on the recorded videos. The photoelastic models were compared regarding their stress intensity (number of fringes) and stress concentration (proximity and location of fringes) under 50N, 100N, 150N and 200N loads. The time taken to reach the 200N load was recorded for each type of specimen. In seeking to compare the stress data obtained, the present study used the same parameter as Ochiai et al. in 2003 (15) and Galvão et al. in 2016 (16), which considered low stress corresponding to the observation of 1 fringe or less, moderate stress when between 1 and 3 fringes were seen, and high stress when more than 3 fringes were detected. The photoelastic models were also compared when the

size and distribution of fringes were similar, allowing to evaluate the load and time necessary to reach a determined size and distribution of the fringes in seeking to check the behavior of the different models during the test (comparison from similarities). For this, the video footage was frozen when the images of fringe patterns of Y-TZP and metal models looked similar to the resin model at 50, 100, 150 and 200N. In order to obtain similarity, color, shape and layout of the fringes were considered.

## RESULTS

The time spent to reach 200N was different for the resin (96 seconds), Y-TZP (112 seconds) and metal (131 seconds). The metal and Y-TZP models reached 50N in 15 seconds, while the resin model took 17 seconds. For the other load intensities registered (100N, 150N and 200N) the resin model has reached first.

Comparing the images obtained from different loads, the metal and Y-TZP models showed larger stress areas. At 50N the larger stress concentration occurred around the apical region of the implant. At 100N Y-TZP and metal crown showed stress at the apical third and at the cervical region, while the resin crown model presented stress at the apical region and at the middle third. At 150N and 200N all models showed tension from the apical to the cervical region, but with greater fringe extension for the Y-TZP and metal models. In general, the Y-TZP and metal



Load (N)	Resin	Y-TZP	CoCr
50	17s	15s	15s
100	44s	46s	49s
150	69s	78s	86s
200	96s	112s	131s

TABLE 1 Time (seconds) spent to reach the loads of 50, 100, 150 and 200N for different models.

Load	Stress Intensity		
	Resin	Y-TZP	Metal
50N	low	moderate	moderate
100N	low	high	high
150N	moderate	high	high
200N	high	high	high

TABLE 2 Stress intensity patterns based on the fringes order for the different materials under different load magnitude (according to the method proposed by Ochiai et al., 2003).

crown models showed higher stress concentration (Fig 4). Regarding the stress intensity, there was some difference between the models. Looking at fringes number and fringes order, while Y-TZP and metal showed similar behavior, resin showed considerable less stress intensity (Table 2). When analyzing the proximity of the fringes, it was evident the higher stress concentration for the metal model, followed by the Y-TZP, while the resin model presented lower concentration of stress around the implant. The analysis of the similarity images showed that the metal crown achieved similarity with the lowest load. For the similarity with 50N in resin it can be observed that the metal and Y-TZP behaved similarly, while at 100N in resin there was a slight difference between the Y-TZP and the metal. For the similarities 1 and 2 (50N and 100N, respectively) the Y-TZP and the metal maintained a ratio of 2:1 with respect to the resin crown. In the similarity 3 (150N) the ratio of difference of the Y-TZP and the metal compared to the resin increased to approximately 3:1. This dynamic analysis showed that to generate similar tensions in the photoelastic resin the metal crown required less load compared to the resin crown, followed by the Y-TZP crown (Fig. 5).

**DISCUSSION**

The null hypothesis was discarded, since there was an influence of the material used to construct the crown on the stress distribution around short dental implants. For all the load intensities applied, the qualitative (visual/

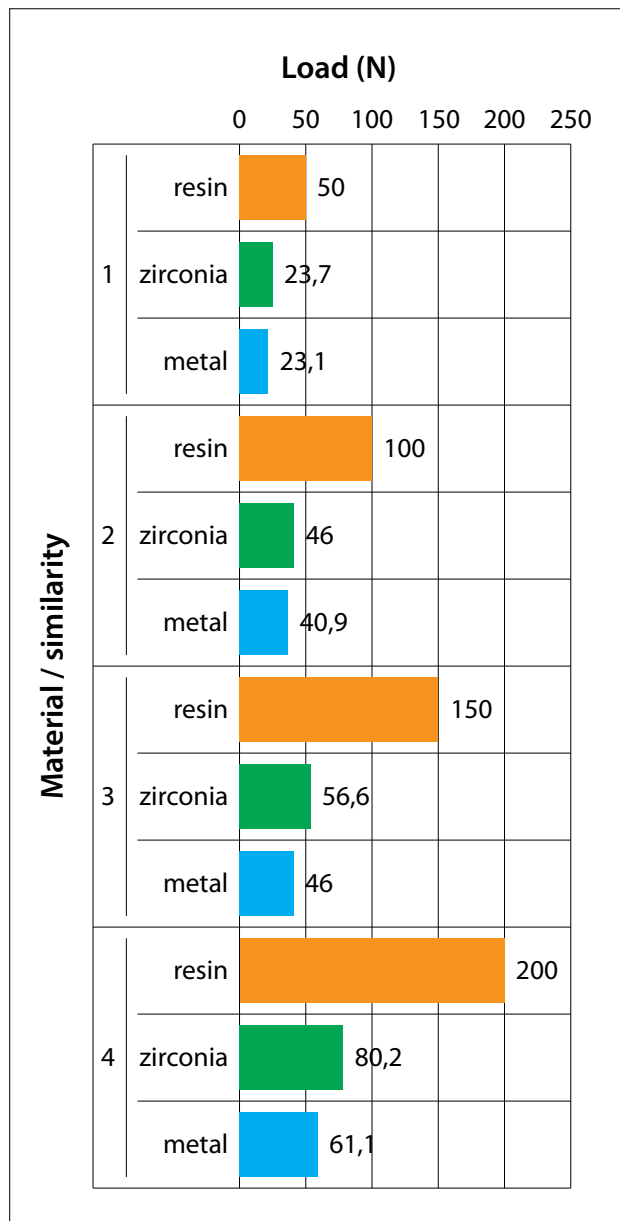


FIG. 5 Graphic presentation plotting the load values for Y-TZP and metal models when it showed similar fringe patterns to resin at 50N (similarity 1), 100N (similarity 2), 150N (similarity 3) and 200N (similarity 4).

subjective) and quantitative comparison between the different kinds of crowns showed the most favorable stress distribution for the resin crown. The same was seen for the similarity test, which demonstrated that metal and Y-TZP models can reach the same stress of resin model under a less intense load.

These results can be explained by the mechanical properties of the materials tested. The acrylic resin has the lower elastic modulus and the higher resilience in relation to CoCr alloy and Y-TZP. Due to this characteristic, the acrylic resin crown, probably, could have suffered higher deformation and load absorption, avoiding the transmittion of stress to other components of the model, including

the peri-implant bone (13–17). The load absorption and deformation can also explain why the resin-based material reached the 200N load earlier than the other models. It should be noted that only an acrylic resin was evaluated in the present study. While this type of material is indicated as provisional/interim restorations some efforts to reinforce it with nanoparticles with the consequence of increasing the fracture toughness, elastic modulus and glass transition temperature (18). With improving these properties, it could be hypothesized that the stress distribution would be affected.

On the other hand, stiffer materials, like CoCr alloy and Y-TZP presented lower and slower deformation and could transmit the stress more intensively to the other parts of the model. The effects of the difference in deformation between resin material, CoCr alloy and ceramics was showed in previous studies (13, 19). However, there are *in vitro* and clinical studies (14, 20) stating that there is no influence of the materials used to construct the crown on the stress around dental implants. It is important to emphasize that these studies used bi-layered prostheses instead of monolithic crowns.

From the clinical aspect, the higher stress concentration around implants can generate microcracks in the peri-implant bone leading to bone resorption (5, 7). It is even more critical for the stress concentration around the collar of the implant. Normally, in cases where the bone volume is reduced and a short dental implant solution is chosen, an unfavorable crown/implant ratio is present, leading to a higher probability of stress concentration in the peri-implant bone (8, 10).

In the present study, the stress concentration initiates from the apical portion of the implant, gradually spreading to the cervical region. It can be attributed to the design of the implant used in the present study, which can contribute to the stress distribution in the bone marrow tissue, thus reducing cervical tension, what would be beneficial for the maintenance of peri-implant bone tissue. The platform switching design of the implant used in the present study can also have contributed to reducing the stress around the cervical third of the implant (21–23).

The present study evaluated qualitatively and quantitatively the stress distribution around short dental implants using a dynamic photoelastic analysis, that allowed a real-time observation of the stress generated. This dynamic analysis allowed the comparison of the materials not only in relation to the fringes formed by the different applied loads, but also in relation to "load moments" where the fringes were similar in all models. The pattern of stress distribution obtained in this study is in accordance to previous studies, which evaluated the stress distribution around locking tapered implants under axial load application and found stresses generated mainly at the apical third of the implant (16, 23).

From the biomechanical aspect, the success of implant supported prosthesis cannot be based only on the stress distribution in the peri-implant bone, once it is just one

factor actuating in a complex system (5, 6, 24). The long-term success of these types of prostheses depends also on the stress distribution in other components like abutment screw, implant and abutment body, veneer material and luting agent (9, 24).

The results of this study can help the clinician to choose the restorative material when the overload is an issue, as in short dental implants with an unfavorable crown/implant ratio, mainly in patients presenting parafunctional habits. However, it is important to interpret the results with caution, since this *in vitro* study has some limitations. The evaluation of stress distribution did not consider the oblique loads, which are more demanding for the peri-implant bone and its excess could lead to bone resorption (1, 23). Another limitation is that the CoCr crown did not receive the porcelain veneer layer, thus it does not represent the real clinical use for this type of restoration. Finally, this study used only one model for each type of crown tested, representing a small sample and, therefore, could have influenced the results.

## CONCLUSION

The material used to construct the crown influenced the stress concentration in the peri-implant bone around locking-tapered short dental implants. The resin crown showed the most favorable stress distribution when compared to Y-TZP and metal (CoCr) crowns.

## REFERENCES

1. Akça K, Çehreli MC. A Photoelastic and strain-gauge analysis of interface force transmission of internal-cone implants. *Int J Periodontics Restorative Dent* 2008;28:391–399.
2. Fugazzotto PA. Shorter implants in clinical practice: rationale and treatment results. *Int J Oral Maxillofac Implants* 2008;23:487–496.
3. Maló P, de Araújo Nobre M, Rangert B. Short implants placed onestage in maxillae and mandibles: a retrospective clinical study with 1 to 9 years of follow-up. *Clin Implant Dent Relat Res* 2007;9:15–21.
4. Annibaldi S, Cristalli MP, Dell'Aquila D et al. Short dental implants: a systematic review. *J Dent Res* 2012;91: 25. doi: 10.1177/0022034511425675.
5. Misch CE, Bidez MW, Sharawy M. A bioengineered implant for a predetermined bone cellular response to loading forces. a literature review and case report. *J Periodontol* 2001;76:1276–1286.
6. Rubo JH, Capello Souza EA. Finite-element analysis of stress on dental implant prosthesis. *Clin Implant Dent Relat Res* 2010;12:105–13. doi: 10.1111/j.1708-8208.2008.00142.x.
7. Frost HM. Presence of microscopic cracks in vivo in bone. *Henry Ford Hosp Med Bull.* 1960;8:25–35.
8. Maminkas J, Puisys A, Kuoppala R, et al. The Prosthetic Influence and Biomechanics on Peri-Implant Strain: a Systematic Literature Review of Finite Element Studies. *J Oral Maxillofac Res.* 2016;7:(e4)1–11.
9. Salvi GE, Bragger U. Mechanical and Technical risks in implant therapy. *Int J Oral Maxillofac Implants* 2009;24(suppl):69–85.
10. Cinar D, Imirzalioglu P. The effect of three different crown heights and two different bone types on implants placed in the posterior maxilla: three-dimensional finite element analysis. *Int J Oral Maxillofac Implants* 2016;31(2):e1–e10. doi: 10.11607/jomi.4048.
11. Urdaneta RA, Daher S, Leary J et al. The survival of ultrashort locking-taper implants. *Int J Oral Maxillofac Implants* 2012;27:644–54.
12. Demiralp, K, Akbulut, N, Kursun, S et al. Survival rate of short, locking taper implants with a plateau design: a 5-year retrospective study. *Biomed Res Int*

- 2015;2015:197451. doi: 10.1155/2015/197451.
13. Çiftçi Y, Canay S. The effect of veneering materials on stress distribution in implant-supported fixed prosthetic restorations. *Int J Oral Maxillofac Implants* 2000;15:571-82.
  14. Santiago Junior JF, Pellizzer EP, et al. Stress analysis in bone tissue around single implants with different diameters and veneering materials: a 3-D finite element study. *Mater Sci Eng C Mater Biol Appl* 2013;33:4700-14.
  15. Ochiai KT, Ozawa S, Caputo AA et al. Photoelastic stress analysis of implant-tooth connected prostheses with segmented and nonsegmented abutments. *J Prosthet Dent* 2003;89:495-502.
  16. Galvão GH, Grossi JA, Zielak JC et al. Influence of metal and ceramic abutments on the stress distribution around narrow implants: a photoelastic stress analysis. *Implant Dent* 2016;25:499-503. doi: 10.1097/ID.0000000000000406.
  17. Davis DM, Rimrott R, Zarb GA. Studies on frameworks for osseointegrated prostheses: Part 2. The effect of adding acrylic resin or porcelain to form the occlusal superstructure. *Int J Oral Maxillofac Implants* 1988;3:275-80.
  18. Topouzi M, Kontonasaki E, Bikiaris D et al. Reinforcement of a PMMA resin for interim fixed prostheses with silica nanoparticles. *J Mech Behav Biomed Mater* 2017;69:213-222. doi: 10.1016/j.jmbbm.2017.01.013.
  19. Grando AF, Rezende CE, Sousa EA et al. Effect of veneering material on the deformation suffered by implant-supported fixed prosthesis framework. *J Appl Oral Sci* 2014;22:209-17.
  20. Teigen K, Jokstad A. Dental implant suprastructures using cobalt-chromium alloy compared with gold alloy framework veneered with ceramic or acrylic resin: a retrospective cohort study up to 18 years. *Clin Oral Implants Res* 2012;23:853-60.
  21. Tabata LF, Rocha EP, Barão VA, Assunção WG. Platform switching: biomechanical evaluation using three-dimensional finite element analysis. *Int J Oral Maxillofac Implants* 2011;26:482-91.
  22. Atieh MA, Ibrahim HM, Atieh AH. Platform switching for marginal bone preservation around dental implants: a systematic review and meta-analysis. *J Periodontol* 2010;81:1350-66.
  23. Pellizzer EP, Carli RI, Falcón-Antenucci RM et al. Photoelastic analysis of stress distribution with different implant systems. *J Oral Implantol* 2014;40:117-22. doi: 10.1563/AAID-JOI-D-11-00138.
  24. Rezende CE, Chase-Diaz M, Costa MD et al. Stress Distribution in single dental implant system: three-dimensional finite element analysis based on an in vitro experimental model. *J Craniofac Surg* 2015;26:2196-200. doi: 10.1097/SCS.0000000000001977.